

A Frequency Reconfigurable U-Shaped Antenna for Dual-Band WIMAX/WLAN Systems

Youcef B. Chaouche^{1, 2, *}, Farid Bouttout³, Mourad Nedil¹,
Idris Messaoudene^{2, 4}, and Ismail Benmabrouk⁵

Abstract—A novel frequency reconfigurable antenna is proposed for WiMAX and WLAN applications. It has a simple structure and compact size of $0.44\lambda_g \times 0.37\lambda_g$. The proposed approach is based on utilizing of a double planar U-shaped antenna. Furthermore, to achieve a reconfigurable function, a PIN diode switch is introduced across the slot between the two U-shaped patches. By controlling the PIN diode, the antenna resonates at two modes of single and dual bands (WiMAX 3.2/3.5 GHz, and WLAN 5.2/5.8 GHz). The obtained gain ranges from 2.3 to 3.9 dBi within the whole operating bands. The simple configuration and low profile nature of the proposed antenna is suitable for Wireless communication systems.

1. INTRODUCTION

Nowadays, satellite and wireless communications have seen a phenomenal level of growth of technology and diversification of services, with enormous research interest in the field of multiband communications [1]. The ever-increasing demands for higher spectral efficiency with high data rate services into a single device maintaining a compact size, pose challenges for many researchers [2]. Therefore, it is necessarily important for the new wireless systems to integrate all these technical requirements. Reconfigurable antennas are crucial components and play a key role in modern wireless communication systems and emerging Internet of Things (IoT) [3]. In fact, antenna reconfigurability can be defined as the dynamic modification of one or more fundamental properties of the antenna in terms of frequency [4], polarization and radiation pattern [5, 6]. Furthermore, the frequency reconfigurability can be achieved by adjusting the effective length of an antenna by using embedded parts such as micro-electromechanical system (RF-MEMS) switches for tuning frequency bands [7], PIN diodes (RF-PIN) [8], or varactor diodes [9] for discrete frequency tuning agility.

In [10], a dual-band frequency-reconfigurable folded slot antenna with an asymmetric structure has been suggested. A dual-band frequency tunable magnetic dipole antenna inserting two varactor diodes to generate 3.5/5.8 WiMAX/WLAN is introduced by Boukarkar et al. in [11]. In [12], a compact reconfigurable patch antenna with frequency diversity for 3G and 4G mobile communication technologies is discussed. In the same area, an E-shaped microstrip patch antenna has been proposed by using simultaneous dual-band reconfigurability [13]. However, these antennas are not compact and use a lot of switches to achieve multiband applications.

In this contribution, a new reconfigurable U-shaped dual-band operation is designed and analyzed. The antenna system has a simple structure, which is composed of double U-shaped resonators with a

Received 10 July 2018, Accepted 3 September 2018, Scheduled 18 September 2018

* Corresponding author: Youcef Braham Chaouche (youcef.brahamchaouche@uqat.ca).

¹ School of Engineering, Wireless Research Underground Laboratory, University of Quebec at Abitibi Temiscamingue, Val d'Or, QC J9P1Y3, Canada. ² Laboratoire d'Electronique et des Télécommunications Avancées, University of Bordj Bou Arreridj, Algeria.

³ LGE Laboratory, M'sila, Department of Electronics, University of Bordj Bou Arreridj, Algeria. ⁴ Ecole Nationale Supérieure d'Informatique (ESI ex. INI), BP 68M, Oued Smar, Algiers, Algeria. ⁵ Al Ain University of Science and Technology, Abu Dhabi, UAE.

PIN diode switch placed in a proper location along the slot to reconfigure the antenna from single to dual-band operation. A prototype of the antenna using BAR 50-02V PIN diode has been fabricated and measured. The overall size of the proposed antenna is $30 \times 25 \text{ mm}^2$ ($0.44\lambda_g \times 0.37\lambda_g$).

2. ANTENNA DESIGN

2.1. Structure and Dimensions

Figure 1 shows the various antenna structures in four steps, which are investigated during the simulation studies, and their reflection coefficients characteristics are plotted and compared in Fig. 2.

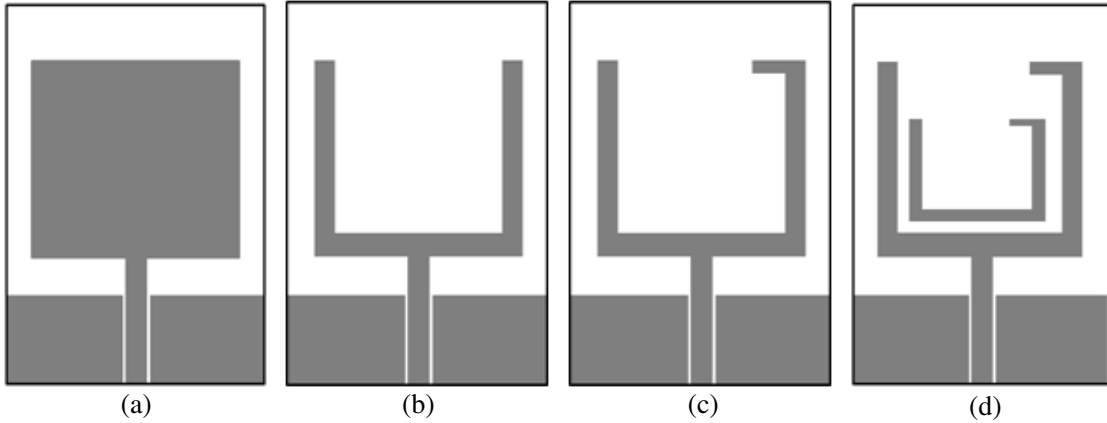


Figure 1. Design evolution of the proposed antenna; (a) Antenna I, (b) Antenna II, (c) Antenna III, and (d) Proposed antenna.

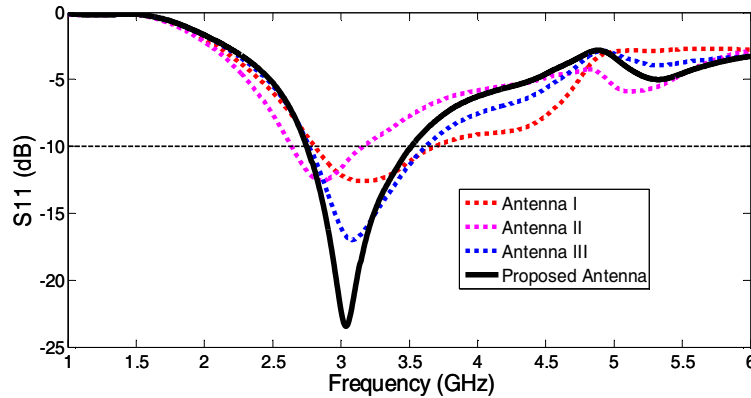


Figure 2. Simulated return losses of various antenna designs.

Figure 1(a) shows the initial model which consists of a rectangle patch with a dimension of $17.6 \times 18.5 \text{ mm}^2$ and a bandwidth of 2.81–3.69 GHz. It can be seen that for the U-shaped patch geometry of Fig. 1(b) a bandwidth of 2.63–3.16 GHz is achieved. On the other hand, Figs. 1(c) and (d) describe the antenna structures after applying the first and second iterations at the edges of the rectangle monopole, with impedance bandwidths of 2.77–3.61 GHz and 2.75–3.52 GHz, respectively. The horizontal tail is designed to get the optimal dimension in terms of return loss and the desired frequency band. Further increase in the iteration order causes only a minor change in the operating bandwidth. In addition, it is observed that the impedance bandwidths of the first-iteration (Fig. 1(c)) and the modified second-iteration (Fig. 1(d)) are almost the same. Fig. 2 illustrates the simulated reflection coefficient for different iterations of the double U-shaped antenna starting from the rectangle geometry as a reference.

It has been illustrated that the validated antenna has a good matching input impedance compared to Antennas I, II and III with a return loss greater than -20 dB. The iteration orders are kept up to the second-iteration.

The geometry of the proposed antenna is shown in Fig. 3. The form of the antenna consists of a double U-shaped monopole printed on a Rogers RO4350B substrate with dielectric constant $\epsilon_r = 3.66$ and loss tangent $\tan \delta = 0.004$.

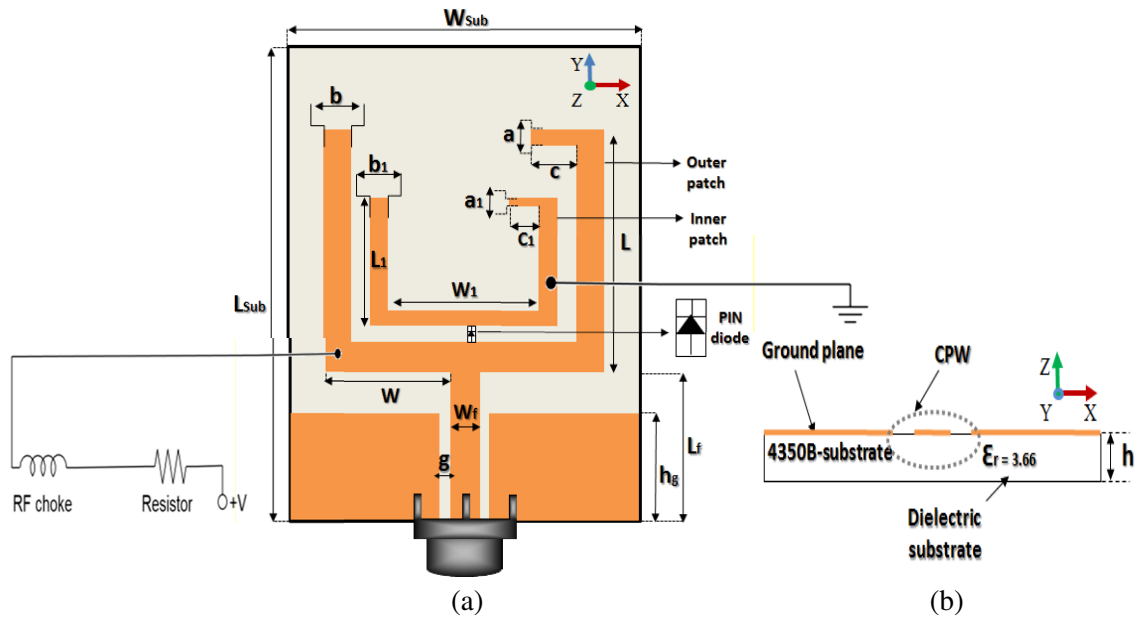


Figure 3. Layout of the proposed antenna. (a) Top view, and (b) side view.

The rectangular radiating patch was cut by a pair of U-shaped slots scaled by a factor equal to 0.6. Two equal finite ground planes, with length h_g are placed symmetrically on both sides of the CPW feed-line. The overall size of the substrate is $L_{sub} \times W_{sub}$ with a thickness of $h = 1.524$ mm. A 50Ω impedance transmission line is connected to the antenna, which consists of a signal strip with a width of W_f centered and connected to a coaxial cable via SMA (Sub-Miniature version A) connector in the feed-line. The parameter G represents the gap between the signal strip and the coplanar ground plane. The antenna was optimized using Ansoft's FEM-based HFSS software [14]. The parameters and dimensions of the antenna are given in Table 1.

Table 1. Parameters of the proposed antenna.

Parameters	Value (mm)	Parameters	Value (mm)
a	1	W_{sub}	25
a_1	0.5	L_{sub}	30
b	2	L_f	8.75
b_1	1.2	W_f	3.6
w	7	G	0.5
w_1	8.16	H_g	6.25
L	17.6	L_1	11.06
c	3.6	c_1	2.08

2.2. Effect of the Horizontal Tail

In this section, a performance analysis concerning the effect of the horizontal tail on the big U-shaped antenna is performed to get low-level reflections at the antenna input and the required standard frequency band. Fig. 4 shows the length effect of the horizontal tail (“ c ” parameter) in terms of return loss. It can be seen from the curve that parameter “ c ” considerably affects the input matching of the antenna. Furthermore, in order to achieve a resonance frequency centered at 3.2 GHz (dedicated to the WiMAX application), the length “ c ” should be optimized ($c = 3.6$ mm).

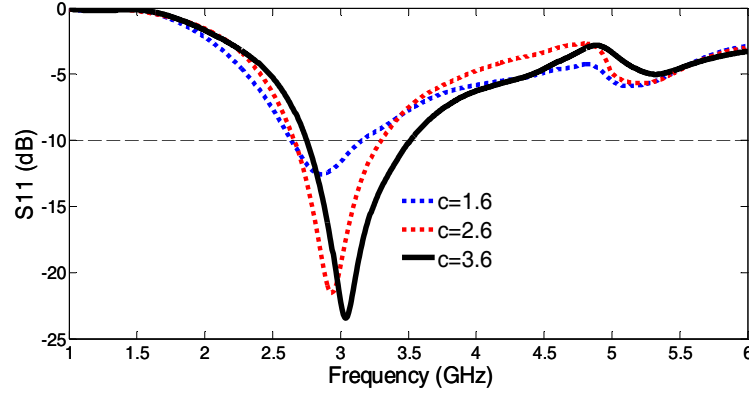


Figure 4. Effect of “ c ” parameter on the reflection coefficients.

2.3. Equivalent Circuit Models of PIN Diode

Beam lead PIN diode (Infineon BAR 50-02V) is used as switching elements to implement electronic reconfigurability. The equivalent circuit models used in the simulation software are illustrated in Fig. 5. According to the PIN diode datasheet [15], a package inductance (L) of 0.6 nH is used for both ON and OFF states. The resistor (R_f) is 4.5 Ω in the forward bias state, and the capacitor (C_T) in the parallel circuit is 0.15 pF for the reverse bias state. The resistor (R_P) is 5 k Ω representing the net dissipative resistance of the diode in the reverse bias state.

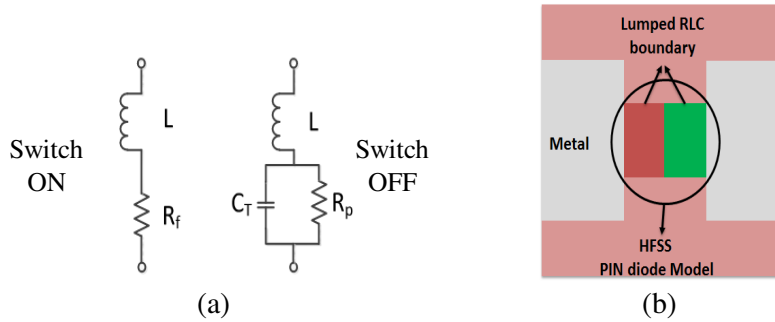


Figure 5. Electrical model of RF PIN diode. (a) Equivalent lumped element model, and (b) HFSS model.

2.4. Current Distributions

The simulated current distributions on the final design antenna at 3.2 GHz and 5.2 GHz are depicted in Fig. 6. When the PIN diode is in OFF state, the frequency band at 3.2 GHz is mainly excited due to the strong current distribution along the big U-shaped boundary curves of the outer patch as shown in Fig. 6(a). As illustrated by Fig. 6(b), the current is mainly localized at the inner and outer patches, exciting the 5.2 GHz resonance mode when the switch is in ON position.

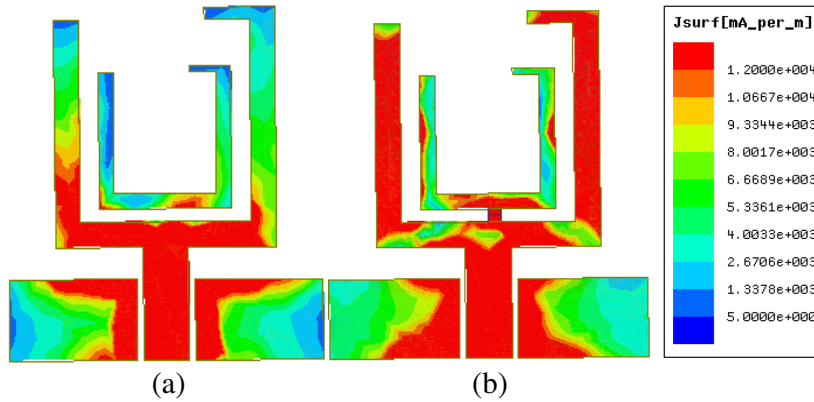


Figure 6. Surface current distribution of proposed antenna at: (a) 3.2 GHz, (b) 5.2 GHz.



Figure 7. The fabricated prototype antenna with bias circuit and experimental setup.

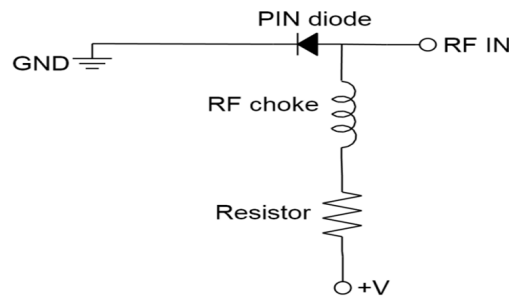


Figure 8. Biasing circuit of the PIN diode.

3. MEASURED RESULTS AND DISCUSSION

The proposed dual-band antenna was designed by using Ansys HFSS software, which is based on the finite element method (FEM). After optimizing the antenna parameters, an experimental prototype of the designed antenna was fabricated to validate the simulated results. A photograph of the manufactured antenna as well as biasing component and wire is shown in Fig. 7. The measurements on the fabricated antenna were carried out using calibrated ANRITSU MS4647A Vector Network Analyzer. In addition, the radiation patterns and gains measurements were performed in an anechoic chamber.

Therefore, the modified geometry is used for frequency reconfigurability (placing the PIN diode and bias line). For independent control of the switch, two 0.3 mm width slots are introduced between

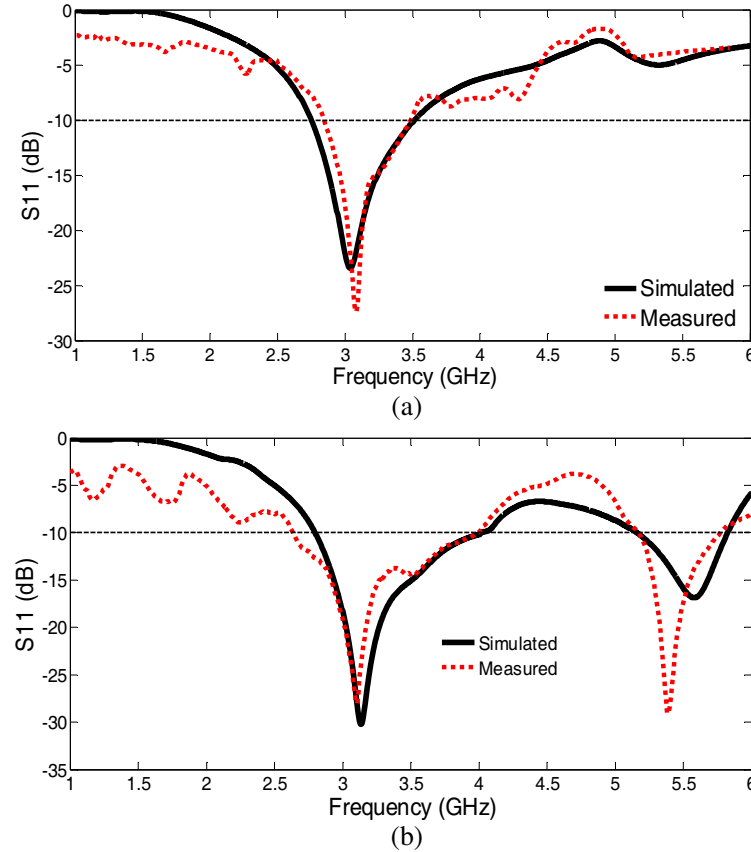
Table 2. Switching mode for the proposed antenna.

Mode	Switch status	Frequency band (GHz)
1. Single band	OFF	3.2
2. Dual band	ON	3.2/3.5/5.2/5.8

the two U-shaped resonators of the antenna in order to provide the isolation necessary between the two ports of the PIN diode. The DC biasing circuit for PIN diode is given in Fig. 8. A $10\ \mu\text{H}$ inductor (from Murata Technology) is used as radio-frequency (RF) choke to keep the RF signal out of the DC bias lines. A resistor of $1\ \Omega$ is mounted on the fabricated antenna, to control the DC biasing current to the PIN-diode. These DC lines are attached to the wires and connected to a DC power supply.

Figure 9 illustrates the simulated and measured S_{11} parameters of the proposed antenna for different switch cases, ON and OFF as listed in Table 2. It can be seen that when PIN diode is turned OFF, a single band 3.2 GHz WiMAX operation with impedance bandwidth from 2.85 to 3.5 GHz is covered. In fact, the proposed antenna operates over both 3.2/3.5 GHz (2.64–4.02 GHz) WiMAX and 5.2/5.8 GHz (5.13–5.85 GHz) WLAN bands, when the diode is turned ON. The small discrepancies between the simulated and measured results is mainly due to the soldering of RF components and also the imperfect DC bias current when the ON state is activated which will degrade the power efficiency and antenna's performance. With these performances, the presented antenna satisfies the requirements of WLAN and WiMAX applications.

The simulated and measured co-polarization far-field radiation patterns on the x - z plane (E -plane)

**Figure 9.** Simulated and measured reflection coefficients of the proposed dual-band antenna: (a) OFF state, and (b) ON state.

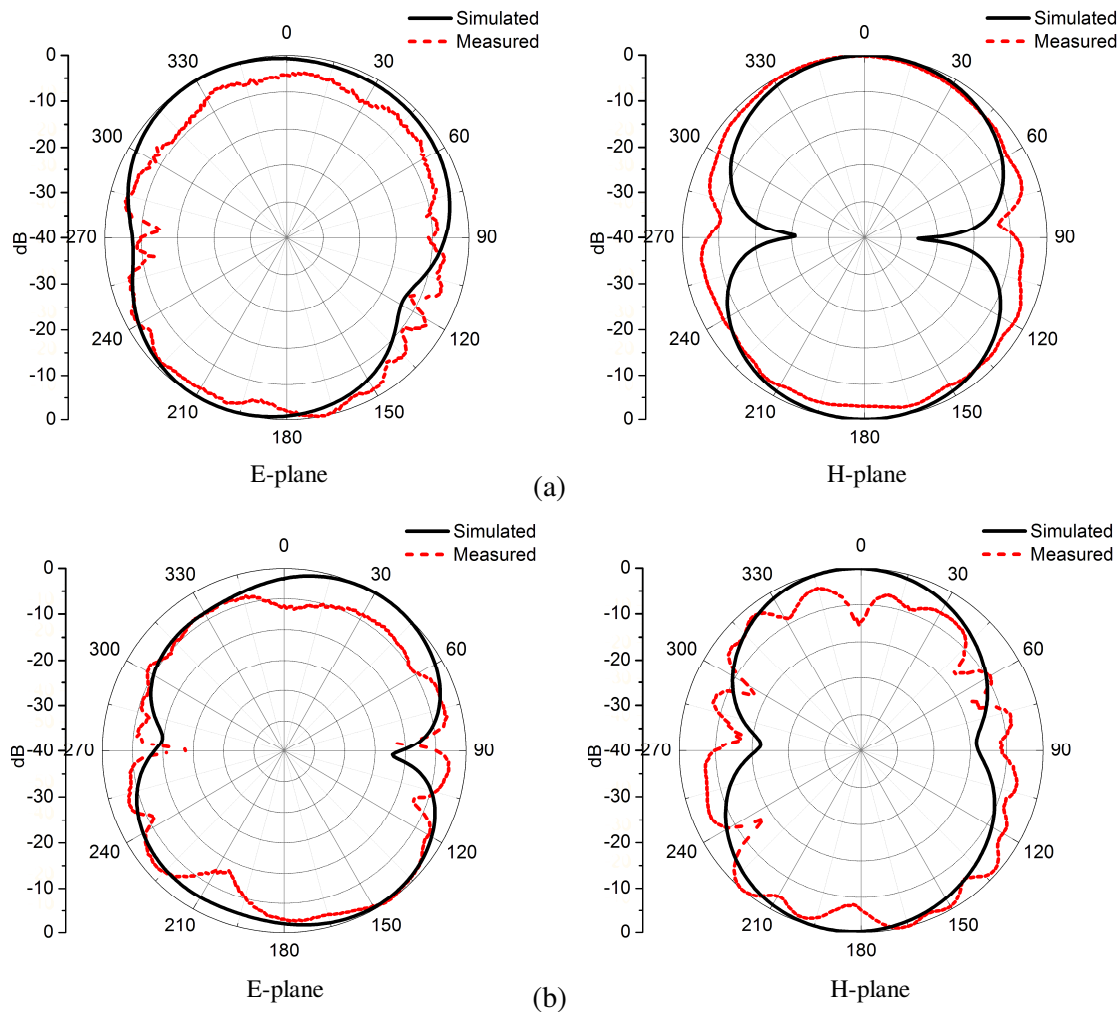


Figure 10. *E* and *H*-plane co-polarization radiation characteristics for the frequencies: (a) 3.2 GHz (OFF state), (b) 5.2 GHz (ON state).

and *y-z* plane (*H*-plane), at two operating frequencies 3.2 GHz (OFF state) and 5.2 GHz (ON state), are shown in Figs. 10(a)–10(b), respectively. From these figures, bidirectional patterns are observed for both *E*-plane and *H*-plane for all operating frequencies. The measured results of co-polarization are almost in good agreement with the simulated ones.

The simulated and measured antenna gains in two states are shown in Fig. 11. The measured realized gain values were taken at the resonance frequency bands of each switched state. It can be observed that the gain responses change with the reconfigurability, and they exhibit different values for different states. From these results, it can be noted that the proposed antenna provides acceptable gains in these operating bands, with a maximum of 2.3 dBi at 3.2 GHz (OFF state), and 3.9 dBi at 5.2 GHz (ON state).

The average simulated and measured gain values and simulated antenna efficiency are summarized in Table 3. As indicated in the table, the measured gain is slightly less than the simulated one in all resonant frequencies, especially in ON state. These reductions may be due to using the series resistance of PIN diode switches in the ON state and also the imperfect DC bias network. It is noted that using PIN diode has a small effect on the gain and efficiency.

Table 4 shows the fabricated antenna compared to the previous antennas reported in the literature [10–13]. This design using one PIN diode provides advantages including simple structure, compact size, low cost, and easy manufacture. One of the additional advantages of this design is that

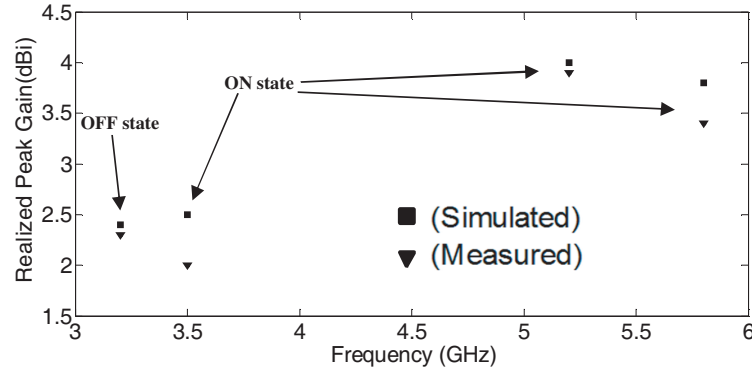


Figure 11. Simulated and measured realized gains for the two modes.

Table 3. Simulated and measured gain and simulated efficiency of the dual-band antenna.

State	Frequency, GHz	Simulated gain, dBi	Measured gain, dBi	Simulated efficiency, %
OFF	3.2	2.4	2.3	94.60
	3.5	2.5	2.0	91.45
ON	5.2	4	3.9	94.39
	5.8	3.8	3.4	88.15

Table 4. Comparison between the fabricated antenna and other reported dual-band antenna.

No.	Antenna	Antenna size ^A	Size reduction (%)	Switching elements types and quantity		Radiation patterns ^B	Frequency range (GHz)
1	Ref. [10]	$0.35\lambda_g \times 0.46\lambda_g \times 0.018\lambda_g$	37.5	PIN diode	3	BID	2.4/3.4/5.2/5.8
2	Ref. [11]	$0.51\lambda_g \times 0.51\lambda_g \times 0.009\lambda_g$	6	Varactor	2	OMNI	3.5/5.8
3	Ref. [12]	$0.40\lambda_g \times 0.34\lambda_g \times 0.013\lambda_g$	55.44	PIN diode	2	UNI	2.1/2.6/4.8
4	Ref. [13]	$0.61\lambda_g \times 0.65\lambda_g \times 0.019\lambda_g$	72.17	PIN diode	3	OMNI	3.1/3.5/7.2/8.1
5	This work	$0.44\lambda_g \times 0.37\lambda_g \times 0.22\lambda_g$	-	PIN diode	1	BID	3.2/3.5/5.2/5.8

^AThe guided wavelength λ_g has been calculated in terms of the lower resonant frequency.

^BBID means bidirectional radiation pattern, while OMNI, and UNI represents omnidirectional, unidirectional radiation pattern, respectively.

it can achieve two configurations with sufficient bandwidths at -10 dB covering full bands of WiMAX 3.2/3.5 GHz, and WLAN 5.2/5.8 GHz.

4. CONCLUSION

This paper has reported an experimental prototype of a CPW dual-band reconfigurable antenna. By introducing double U-shaped resonators and by altering the operating modes of the PIN diode, a dual-band antenna operating at WiMAX and WLAN bands has been achieved successfully. The radiation pattern results are fairly bidirectional in both E - and H -planes for both modes with an optimum gain about 2.3–3.9 dBi. This antenna has a good potential for WiMAX 3.2/3.5 GHz and WLAN 5.2/5.8 GHz systems.

ACKNOWLEDGMENT

The authors would like to acknowledge the support of the National Institute of Scientific Research (INRS-EMT), University of Quebec, Canada. They would also like to thank Pr. Tayeb A. Denidni for the use of their antenna pattern measurement system.

REFERENCES

1. Zhang, L., T. Jiang, and Y. Li, "Dual-band printed antenna for WLAN applications," *PIERS Proceedings*, 1020–1023, Prague, Czech Republic, July 6–9, 2015.
2. Yasir, L. A., A. O. George, S. A. Abdulkareem, J. M. Husham, A. A. Ramzy, A. A. A. Raed, and M. N. James, "Design of frequency reconfigurable multiband compact antenna using two PIN diodes for WLAN/WiMAX applications," *IET Microwaves, Antennas & Propagation*, Vol. 11, No. 8, 1098–1105, 2017.
3. Braham Chaouche, Y., F. Bouttout, I. Messaoudene, L. Pichon, M. Belazzoug, and F. Chetouah, "Design of reconfigurable fractal antenna using pin diode switch for wireless applications," *16th Mediterranean Microwave Symposium (MMS'16)*, November 14–16, 2016.
4. Han, L., C. Wang, et al., "Compact frequency-reconfigurable slot antenna for wireless application," *IEEE Antennas Wirel. Propag. Lett.*, Vol. 15, 1795–1798, 2016.
5. Shi, S., W. P. Ding, and K. Luo, "A monopole antenna with dual-band reconfigurable circular polarization," *Progress In Electromagnetics Research C*, Vol. 55, 35–42, 2014.
6. Trong, N. N., L. Hall, and C. Fumeaux, "A dual-band dual pattern frequency reconfigurable antenna," *Microw. Opt. Technol. Lett.*, Vol. 59, 2710–2715, 2017.
7. Yamagajo, T. and Y. Koga, "Frequency reconfigurable antenna with MEMS switches for mobile terminals," *Antennas and Propagation in Wireless Communications (APWC)*, 1213–1216, 2011.
8. Mansoul, A., F. Ghanem, M. R. Hamid, E. Salonen, and M. Berg, "A bandwidth reconfigurable antenna with a fixed lower and a variable upper limit," *IET Microwaves, Antennas & Propagation*, Vol. 10, No. 15, 1725–1733, 2016.
9. Lim, J.-H., G.-T. Back, Y.-I. Ko, C.-W. Song, and T.-Y. Yun, "A reconfigurable PIFA using a switchable PIN-diode and a fine-tuning varactor for USPCS/WCDMA/m-WiMAX/WLAN," *IEEE Transactions on Antennas and Propagation*, Vol. 58, No. 7, 2404–2411, 2010.
10. Chen, G., X. L. Yang, and Y. Wang, "Dual-band frequency-reconfigurable folded slot antenna for wireless communications," *IEEE Antennas Wirel. Propag. Lett.*, Vol. 11, 1386–1389, 2012.
11. Boukarkar, A., X. Lin, and Y. Jiang, "A dual-band frequency-tunable magnetic dipole antenna for WiMAX/WLAN applications," *IEEE Antennas Wirel. Propag. Lett.*, Vol. 15, 492–495, 2016.
12. Bekali, Y. K. and M. Essaaidi, "Compact reconfigurable dual frequency microstrip patch antenna for 3G and 4G mobile communication technologies," *Microwave and Optical Technology Letters*, Vol. 55, No. 7, July 2013.
13. Asif, S. M., A. Iftikhar, S. M. Khan, M. Usman, and B. D. Braaten, "An E-shaped microstrip patch antenna for reconfigurable dual-band operation," *Microwave and Optical Technology Letters*, Vol. 58, 1485–1490, 2016.
14. Ansoft Corporation, HFSS, High frequency structure simulator version 15, Finite element package, Ansoft Corporation, Available at: <http://www.ansoft.com>.
15. Datasheet for Infineon BAR50-02V, Silicon PIN Diode, Infineon Technologies AG. <http://www.farnell.com/datasheets/1500311.pdf>.